

Seasonal Dynamics and Safety Assessment of Physicochemical and Heavy Metal Parameters in Jega River, Kebbi State, Nigeria

Abubakar Isah ¹, Israel Obaroh ², Sani Abdulrahman ³ and Tajudeen Yahaya ^{3,*}

¹ Department of Science Laboratory Technology, Umar Ali Shinkafi Polytechnic, Sokoto, PMB 2356, Sokoto State, Nigeria

² Department of Biological Sciences, Kampala International University, Kampala P.O. Box 20000, Uganda

³ Department of Biological Sciences, Federal University Birnin Kebbi, Birnin Kebbi, PMB 1157, Kebbi State, Nigeria

* Correspondence: yahaya.tajudeen@fubk.edu.ng or yahayatajudeen@gmail.com

How To Cite: Isah, A.; Obaroh, I.; Abdulrahman, S.; et al. Seasonal Dynamics and Safety Assessment of Physicochemical and Heavy Metal Parameters in Jega River, Kebbi State, Nigeria. *Glob. Environ. Sci.* **2026**, *2*(2), 208–223. <https://doi.org/10.53941/ges.2026.100014>

Publication History

Received: 14 February 2026

Revised: 18 April 2026

Accepted: 22 April 2026

Published: 19 May 2026

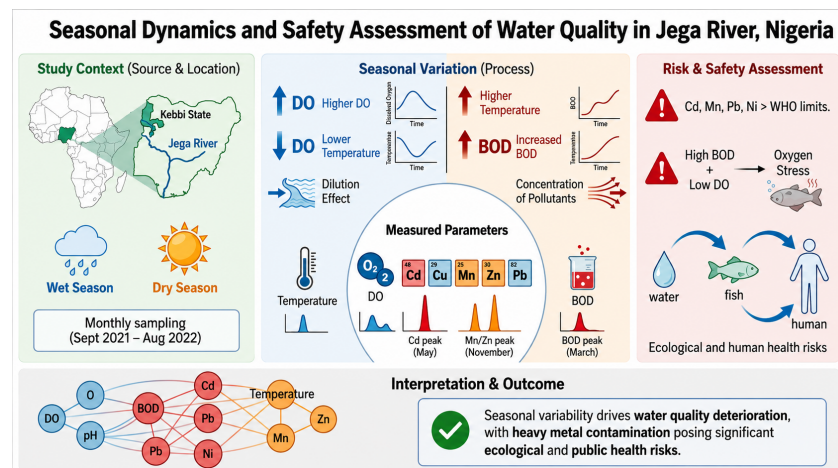
Keywords

dissolved oxygen (DO);
Jega River;
heavy metals; lead (Pb);
physicochemical parameters

Highlights

- Jega River exhibited significant seasonal variation ($p < 0.05$) in physicochemical parameters and heavy metal over the one-year study.
- Water temperature ranged from 27.71 °C (August) to 32.00 °C (May), DO peaked in July (7.47 mg/L) and dropped to its lowest in March (2.73 mg/L). BOD reached a critical maximum in March (43.60 mg/L).
- Heavy metals showed notable peaks: Cd (0.627 mg/L, May), Cu (0.051 mg/L, April), Mn (0.73 mg/L, November), and Zn (0.14 mg/L, November).
- Concentrations of Cd, Mn, Ni, Pb, along with DO and BOD levels, exceeded WHO permissible limits.

Abstract: Jega River in Kebbi State, Nigeria, is an important freshwater resource that supports diverse ecosystem functions. Despite its significance, recent comprehensive assessments of its water quality are lacking. This study evaluated the safety and seasonal variation of physicochemical parameters and heavy metal concentrations over a one-year period. Water samples were collected monthly between September 2021 and August 2022 and analyzed following standard protocols. The results revealed statistically significant ($p < 0.05$) seasonal variations in most parameters. For instance, water temperature peaked in May (32.00 ± 0.58 °C) and was lowest in August (27.71 ± 0.33 °C), reflecting seasonal thermal fluctuations. DO levels were highest in July (7.47 ± 0.20 mg/L) and lowest in March (2.73 ± 0.00 mg/L), while BOD reached its maximum levels in March (43.60 ± 4.45 mg/L). Among the heavy metals, Cd exhibited the highest concentration in May (0.627 ± 0.05 mg/L), Cu peaked in April (0.051 ± 0.00 mg/L), Mn was highest in November (0.73 ± 0.20 mg/L), and Zn reached its maximum concentrations in November (0.14 ± 0.00 mg/L). Notably, concentrations of Cd, Mn, Ni, and Pb, as well as DO and BOD, exceeded the World Health Organization (WHO) permissible limits for surface water. This indicates potential risks to both aquatic organisms and human health. Correlation analysis showed strong positive and negative relationships among several parameters, suggesting common pollution sources and complex interactions. Overall, these findings provide valuable data for water quality monitoring, pollution control strategies, and sustainable water resource management in line with national policies.



1. Introduction

Water is an essential component of life, and its absence makes life unsustainable. It is a fundamental natural resource that has significantly influenced the development and distribution of human settlements over time [1]. Water and water resources are crucial not only for sustaining life but also for ensuring food security and maintaining productive ecosystems. In the human body, water plays multiple critical roles, including serving as a structural component, a universal solvent, a medium and reactant for biochemical reactions, a transporter of nutrients and waste, a regulator of body temperature, and a lubricant and shock absorber [2].

Humans primarily meet their water needs from freshwater sources such as rivers, lakes, and streams, which constitute less than 3% of the Earth's total water and less than 1% of the readily accessible freshwater [3]. With rapid population growth, urbanization, industrialization, and agricultural expansion, these freshwater sources face increasing stress and pollution [4]. The intensification of human activities has led to the degradation of water quality, particularly through the discharge of pollutants into surface water systems [5]. Additionally, natural factors such as soil composition, topography, and weathering processes can contribute to water contamination [6].

Pollutants affect key water quality parameters, including pH, temperature, nutrient levels, salinity, dissolved oxygen, biochemical and chemical oxygen demand (BOD and COD), turbidity, and flow velocity [7]. Elevated concentrations of total suspended and dissolved solids, total alkalinity, and acidity further degrade water quality [8]. Such disruptions can lead to ecological imbalances, rendering water unfit for human consumption and adversely affecting aquatic organisms like fish, crabs, and other biodiversity [6]. Ultimately, water pollution compromises the ecological, cultural, and economic functions of water bodies, including fishing, farming, transportation, and domestic use.

Among the most concerning pollutants in aquatic ecosystems are heavy metals, which are introduced into water bodies through various natural and anthropogenic sources such as industrial effluents, agricultural runoff, domestic wastewater, urban stormwater, landfill leachates, and atmospheric deposition [9]. Heavy metals are defined as metallic elements with relatively high atomic weights and densities that are toxic even at low concentrations [10]. Key heavy metals of environmental concern include mercury (Hg), cadmium (Cd), arsenic (As), chromium (Cr), thallium (Tl), lead (Pb), copper (Cu), manganese (Mn), zinc (Zn), and nickel (Ni). Although naturally occurring in the Earth's crust, their increased concentrations in aquatic systems are primarily due to anthropogenic activities. Unlike organic pollutants, heavy metals are non-biodegradable, possess long biological half-lives, and tend to bioaccumulate in the tissues of

living organisms [11]. Through bioaccumulation and biomagnification, these metals can concentrate along the food chain, leading to toxic effects in organisms far removed from the initial contamination source. Humans can be exposed to heavy metals through ingestion of contaminated water and food, inhalation of polluted air, and dermal absorption [12]. At toxic levels, many heavy metals exhibit carcinogenic, immunotoxic, neurotoxic, and mutagenic properties [13]. Health effects associated with heavy metal exposure include cardiovascular, gastrointestinal, reproductive, neurological, muscular, and genetic disorders. Specific conditions such as eyelid edema, nasal and pharyngeal congestion, tumors, and systemic toxicity are particularly linked to Cd, Cr, and Pb exposure [10]. Although the potential detrimental effects of heavy metal-polluted water on the quality of receiving water bodies are numerous, their risk effects may depend on the volume and composition of the effluent that has been discharged [14].

Given the risks associated with contaminated water, continuous monitoring of water quality is imperative to protect public health and preserve ecological integrity. In Kebbi State, northwestern Nigeria, the Jega River serves multiple vital ecosystem services, including drinking and domestic water supply, washing, fishing, transportation, and dry-season irrigation. However, these activities may be polluting the river, as noticed in its color. Despite this threat, the safety of the river's water has not been evaluated in recent times. This may cause ecological risks and health challenges to humans. Additionally, the river discharges directly into the River Niger, a major river in Nigeria that serves many communities across the north-south divide of the country. Thus, ecological and health risks of the river may have a multiplier effect in the country. Assessing the ecological and health safety of the river's water is imperative to prevent unintended fatality and keep the river functioning. This study was therefore designed to assess the safety of the river through physicochemical parameters and heavy metal concentrations assessment of the river's water. The findings aim to inform water safety management and contribute to achieving Sustainable Development Goals (SDGs) 6.3, which aims to improve water quality by reducing pollution, eliminating dumping, and minimizing the release of hazardous chemicals and materials [15].

2. Materials and Methods

2.1. Description of the Study Sites

This study was carried out on the Jega River, located in the Jega Local Government Area of Kebbi State, in northwestern Nigeria (Figure 1). The area lies between Latitude 12°13'19.88" N and Longitude 4°22'46.67" E. The vegetation is predominantly savannah grassland, interspersed with umbrella-shaped trees and shrubs typical of the Sudan savannah zone. The climate in Jega is

characterized by a distinct dry and wet season. The dry season typically extends from November to May, while the rainy season spans from June to October. Additionally, the area experiences the Harmattan, a dry, dusty wind from the Sahara Desert between November and February, often accompanied by low humidity and reduced visibility. During the hot season (March to June), daytime temperatures can exceed 40 °C, while during the Harmattan period (December to February), temperature may drop below 20 °C, especially in the early morning hours. The inhabitants of Jega are predominantly of Hausa and Fulani ethnic groups, with livelihoods primarily centered on subsistence and commercial farming, fishing, trading, and traditional crafts. The community also includes Igbo and

Yoruba settlers who are mainly involved in trading and artisanal activities, respectively.

The Jega River originates within the Jega Local Government Area and serves as the principal watercourse in the town, eventually discharging into the River Niger. The river is underlain by Precambrian basement complex rocks with overlying alluvial deposits. Its soils are mainly ferruginous and alluvial, prone to erosion and suitable for farming. The Jega River plays a vital role in supporting the local economy and daily life, serving as a source for domestic water use, washing, fishing, irrigation, and livestock grazing. However, these anthropogenic activities along the riverbanks may be contributing to its degradation, as evidenced by visible changes in water colour and a possible decline in water quality.

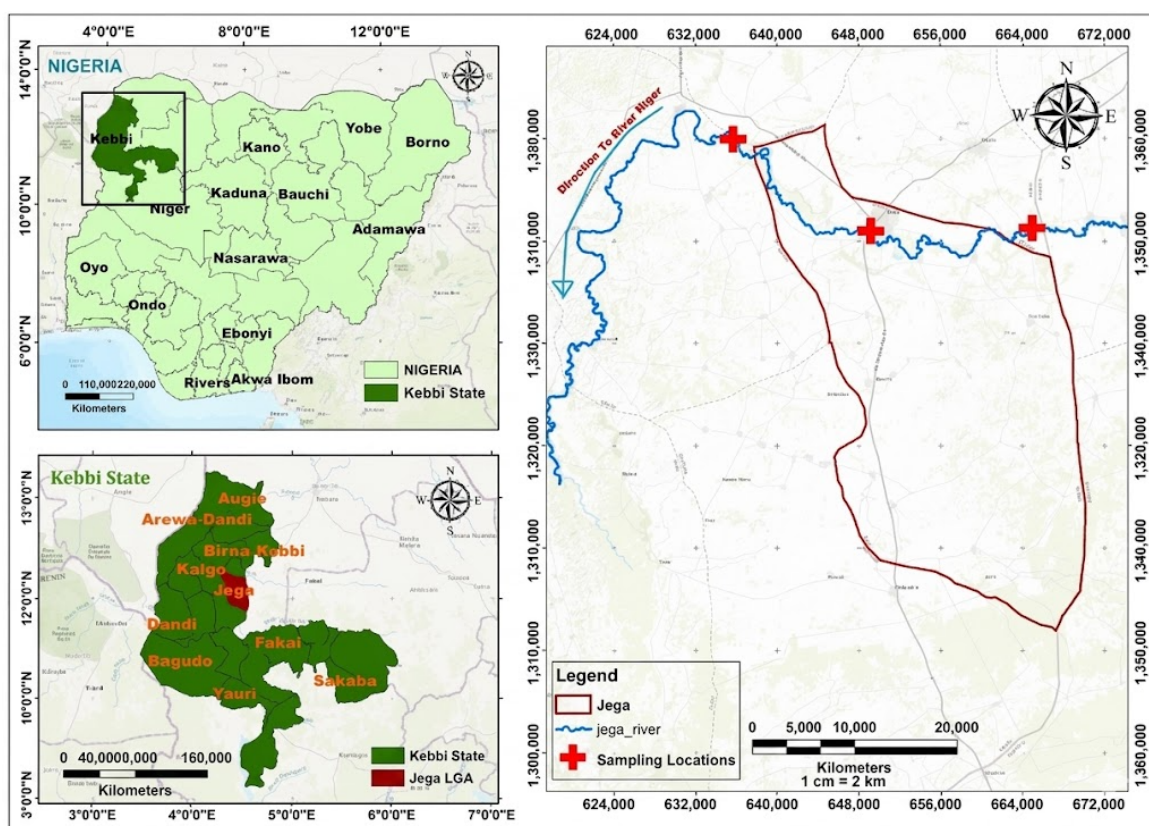


Figure 1. Map of the study area.

2.2. Sample Collection

Water samples were collected monthly over a 12-month period (September 2021–August 2022) to capture seasonal variations in water quality during both the rainy and dry seasons. Sampling was carried out at three designated points along the Jega River: upstream (~5 km before Jega town), midstream (within Jega town), and downstream (~5 km after Jega town). These locations were chosen to provide a spatial representation of water quality and to capture potential variations arising from natural processes and human activities around Jega town.

At each location, water samples were collected randomly using clean, pre-rinsed 1000 mL polyethylene

terephthalate (PET) bottles. The bottles were immediately sealed to prevent contamination and wrapped in opaque black polyethylene bags to minimize light exposure. Samples were transported in an ice-filled box to the laboratory and stored at 4 °C until analysis. Each month, three samples from each location (nine in total) were pooled, resulting in 108 samples over the study period (12 months × 9 samples).

At each sampling location, three replicate samples were collected and composited to form a single representative sample per site. The composited samples from the three sites were then averaged to obtain a monthly value representing overall river water quality. While this approach enhances

representativeness at the river scale, it may reduce the resolution of site-specific variability.

2.3. Determination of Physicochemical Parameters

Physicochemical parameters were analyzed following the standard procedures of the American Public Health Association [16]. Time-sensitive parameters such as temperature, pH, total dissolved solids (TDS), alkalinity, and acidity were measured on-site. Temperature was determined with a liquid-in-glass thermometer; TDS with an HM Digital TDS Meter (Model TDS-4, HM Digital, Inc., Torrance, CA, USA); and pH with a Pye Unicam pH meter (Pye Unicam Ltd., Cambridge, UK). In the laboratory, a DR 2000 spectrophotometer (Model 50150, Hach Company, Loveland, CO, USA) was used to analyze carbonate (CO_3^{2-}), bicarbonate (HCO_3^-), calcium (Ca^{2+}), and magnesium (Mg^{2+}). Chloride (Cl^-) concentrations were determined using an Avial chloride meter (20 × 40 mm, Avial, Gloucestershire, UK). Water hardness was measured by complexometric titration with ethylenediaminetetraacetic acid (EDTA). Turbidity was assessed with a calibrated turbidimeter, and electrical conductivity with a standard EC meter. Dissolved oxygen (DO) and biological oxygen demand (BOD) were measured using a DO meter (Model H12400, Hanna Instruments, Woonsocket, RI, USA) following standard incubation and measurement protocols.

2.4. Determination of Heavy Metals

The concentrations of heavy metals in the water samples were determined using Atomic Absorption Spectrophotometry (AAS), following a modified protocol adapted from Yahaya et al. [1]. The procedure involved three main steps: sample digestion, preparation of standard solutions, and instrumental analysis.

2.4.1. Sample Digestion

Five milliliters (5 mL) of each water sample were transferred into a clean 100-mL beaker. To this, 25 mL of freshly prepared 70% aqua regia (a mixture of concentrated nitric acid [HNO_3] and hydrochloric acid [HCl] in a 1:3 ratio) and 5 mL of diluted hydrogen peroxide (H_2O_2) were added. The mixture was gently heated at 79 °C until digestion was complete, then allowed to cool at room temperature. The digested solution was filtered into a 50-mL volumetric flask and diluted to the mark with deionized water.

A blank sample was prepared using distilled deionized water and digested in the same manner as the test samples. A portion of the digested sample solution was then used for further analysis and preparation of calibration standards.

2.4.2. Preparation of Standard Solutions

High-purity standard stock solutions (1000 mg/L) of each metal were used to prepare working standards.

Calibration standards were prepared using serial dilutions to achieve concentrations within the linear detection range of each metal. The dilution formula used was $C_1V_1 = C_2V_2$.

Where:

- C_1 = concentration of stock solution
- V_1 = volume of stock solution required
- C_2 = desired concentration of working solution
- V_2 = final volume of the working solution

Preparation details for each metal standard are as follows:

- Lead (Pb): Aliquots of 0.2, 0.4, 0.6, 0.8, and 1.0 mL of the stock solution were each diluted to 100 mL with distilled water, yielding final concentrations of 2.0, 4.0, 6.0, 8.0, and 10.0 mg/L.
- Cadmium (Cd): 1 mL of the stock solution was diluted to 100 mL to obtain a 10 mg/L intermediate solution. From this, 0.2, 0.4, 0.6, 0.8-, and 1.0-mL aliquots were further diluted to 100 mL to obtain final concentrations of 0.02, 0.04, 0.06, 0.08, and 0.1 mg/L.
- Copper (Cu): 0.2, 0.4, 0.6, 0.8, and 1.0 mL of the stock solution were each diluted to 100 mL with distilled water to obtain concentrations of 2.0, 4.0, 6.0, 8.0, and 10.0 mg/L.
- Zinc (Zn): 0.2, 0.4, 0.6, 0.8, 1.0, and 1.2 mL of the stock solution were diluted to 100 mL to obtain final concentrations of 0.2, 0.4, 0.6, 0.8, 1.0, and 1.2 mg/L.
- Iron (Fe): An intermediate solution of 100 mg/L was prepared by diluting 10 mL of stock solution with 90 mL of distilled water. Working standards of 0.5, 1.0, 1.5, 2.0, and 2.5 mg/L were then prepared by diluting 0.5, 1.0, 1.5, 2.0, and 2.5 mL of the intermediate solution to 100 mL.
- Chromium (Cr): A 1000 mg/L stock solution was prepared by dissolving 0.2133 g of chromium (III) nitrate nonahydrate ($\text{Cr}(\text{NO}_3)_3 \cdot 9\text{H}_2\text{O}$) in a small volume of distilled water with a few drops of concentrated nitric acid. The solution was transferred to a 1-L volumetric flask and diluted to volume with distilled water.
- Manganese (Mn): A 1000 mg/L stock solution was prepared by dissolving 0.3193 g of manganese (II) sulfate monohydrate ($\text{MnSO}_4 \cdot \text{H}_2\text{O}$) in distilled water and making up the volume to 1 L.
- Nickel (Ni): A 1000 mg/L stock solution was prepared by dissolving 0.2383 g of nickel (II) sulfate hexahydrate ($\text{NiSO}_4 \cdot 6\text{H}_2\text{O}$) in distilled water and diluting to 1 L.

Each solution was thoroughly mixed and labeled with the metal name, concentration, and date of preparation.

2.4.3. Instrumental Analysis

Heavy metal concentrations in the digested samples were determined using a PG Atomic Absorption Spectrophotometer (AAS) (Model AA990, PG Instruments Ltd., Lutterworth, UK). The instrument was equipped with element-specific hollow cathode lamps. An air-acetylene flame was used as the fuel-oxidant system, with air as the

support gas. Calibration curves were established for each metal using the prepared working standards, and sample concentrations were derived by comparing their absorbance readings to the calibration plots.

2.5. Quality Control and Assurance

To ensure the reliability and accuracy of analytical results, strict quality control and assurance protocols were followed throughout the study. Only analytical-grade reagents and chemicals were used for all procedures.

All glassware and plastic containers were thoroughly decontaminated prior to use. This was achieved by soaking them in concentrated nitric acid (HNO₃) for 24 h, followed by multiple rinses with ultrapure deionized water to eliminate any residual contaminants. To prevent the introduction of extraneous metals, all sample handling and processing were conducted without contact with metal-based instruments or surfaces.

Blank samples (prepared using ultrapure water) were analyzed periodically alongside the test samples to monitor and correct for potential background contamination. Each sample was analyzed in triplicate, and the reproducibility of results was confirmed by ensuring minimal variation among the replicate measurements.

2.6. Data Analysis

The data obtained from the water samples were analyzed using both descriptive and inferential statistical techniques. Descriptive statistics, including the mean, standard deviation, and range, were employed to summarize and compare water quality parameters across the wet and dry seasons. One-way Analysis of Variance (ANOVA) was employed to assess significant differences in physicochemical parameters and heavy metal concentrations across months. Where significant differences were observed ($p < 0.05$), Tukey's Honestly Significant Difference (HSD) post-hoc test was applied to separate means. Superscripts (a, b, c) were used to denote statistically significant differences among group means. All statistical analyses were performed using IBM SPSS.

Additionally, correlation analysis was used to examine relationships among various water quality parameters, as well as their associations with potential external influences such as rainfall and agricultural activities. Seasonal trends and patterns in the data were further explored through graphical representations, allowing for visual comparison of variations in water quality parameters over time.

3. Results

3.1. Physicochemical Parameters of the Water Samples

The mean values of the physicochemical parameters of the water samples are presented in Table 1. The water temperature was highest in May, with a mean value of 32.00 ± 0.58 °C, while the lowest mean temperature was

recorded in August, at 27.71 ± 0.33 °C. The pH was highest in September, with a mean value of 7.00 ± 0.10 , whereas the lowest pH values were observed in October and February, both at 6.50 ± 0.10 and 6.50 ± 0.03 , respectively. Electrical conductivity (EC) reached its highest in March, with a mean value of 140.20 ± 0.60 µS/cm, while the lowest value was observed in September, with a mean of 84.90 ± 9.70 µS/cm. Dissolved oxygen (DO) levels peaked in July at 7.47 ± 0.20 mg/L, and the lowest levels were recorded in October and March, both at 2.73 ± 0.00 mg/L. Biochemical oxygen demand (BOD) was highest in March, with a mean value of 43.60 ± 4.45 mg/L, and lowest in September, at 21.50 ± 0.64 mg/L. Carbonate (CO₃) concentrations were highest in March, with a mean of 7.60 ± 0.17 mg/L, and lowest in December, where the concentration was 0.00 ± 0.00 mg/L. Bicarbonate (HCO₃) showed the highest mean value in August at 90.71 ± 1.33 mg/L, while the lowest value was recorded in November, at 16.50 ± 1.78 mg/L. Chloride (Cl) was highest in February, with a mean of 3.50 ± 1.37 mg/L, and lowest in November, where it was 0.00 ± 0.00 mg/L. Calcium (Ca) levels were highest in July, with a mean of 85.30 ± 3.53 mg/L, while the lowest value was observed in September, at 24.00 ± 3.15 mg/L. The highest concentration of magnesium (Mg) was recorded in May, with a mean value of 36.40 ± 2.12 mg/L, while the lowest concentration was observed in October, with a mean value of 6.76 ± 0.00 mg/L. Total dissolved solids (TDS) were highest in September, with a mean value of 5.67 ± 0.33 mg/L, and lowest in April, with a mean value of 1.53 ± 0.50 mg/L. Significant differences ($p < 0.05$) were observed in all the parameters studied.

3.2. Concentrations of Heavy Metals in the Water Samples

The mean values of heavy metals in the water samples are shown in Table 2. Cadmium (Cd) concentrations were highest in May, with a mean value of 0.627 ± 0.05 mg/L, while the lowest concentration was recorded in June, with a mean value of 0.013 ± 0.01 mg/L. Copper (Cu) levels were highest in May, with a mean of 0.6 ± 0.02 mg/L, while the lowest concentration was observed in June, at 0.01 ± 0.01 mg/L. Chromium (Cr) was highest in January, with a mean value of 0.06 ± 0.00 mg/L, while the lowest concentration was recorded in March, April, and May, each with a mean value of 0.01 ± 0.00 mg/L. Iron (Fe) was highest in December, with a mean value of 1.4 ± 0.13 mg/L, while the lowest concentration was recorded in February, at 0.17 ± 0.01 mg/L. Manganese (Mn) reached its highest level in November, with a mean value of 0.73 ± 0.2 mg/L, while the lowest levels were observed in July and August, each with a mean of 0.1 ± 0.01 mg/L. Nickel (Ni) had its highest concentrations in September, October, and February, with a mean value of 0.1 ± 0.01 mg/L, while the lowest levels were recorded in the remaining months.

Lead (Pb) was highest in February, with a mean value of 0.10 ± 0.00 mg/L, while the lowest levels were observed in September, October, November, December, and January. Zinc (Zn) was highest in November, with a mean value of 0.14 ± 0.00 mg/L, while the lowest concentrations were observed in the other months. Significant differences ($p < 0.05$) were observed in most of the parameters studied.

3.3. Seasonal Trend Decomposition (STL) of Selected Physicochemical Parameters of Jega River

Figure 2 shows the STL decomposition of dissolved oxygen (DO) levels over time, separating the time series into trend, seasonal, and residual components. The trend

indicates a general upward movement in DO levels, especially noticeable from early 2021 to mid-2022. The seasonal component reveals recurring fluctuations across months, while the residuals appear to be randomly distributed, suggesting that the STL model has effectively captured the main patterns in the DO data.

Figure 3 below illustrates the STL decomposition of pH levels over time into trend, seasonal, and residual components. The trend component shows a gradual increase in pH levels, indicating a long-term shift toward more alkaline conditions. The seasonal pattern is relatively stable with slight oscillations, and the residuals are minimal and randomly dispersed, suggesting that the model has successfully isolated the key temporal patterns in the pH data.



Figure 2. STL plot for the decomposition of dissolved oxygen (DO).

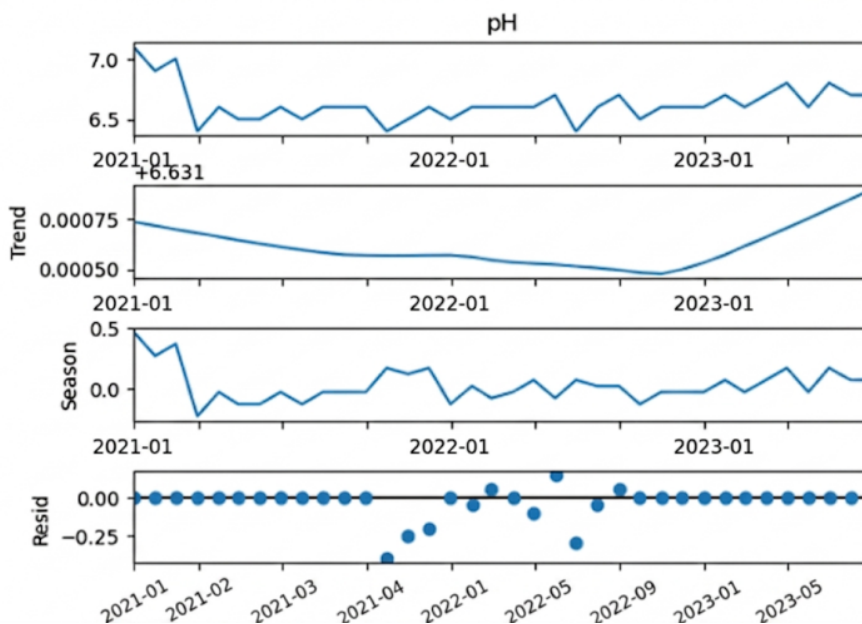


Figure 3. STL plot for the decomposition of pH Levels.

Table 1. Monthly concentrations of the physicochemical parameters of the water samples.

Months	T (°C)	pH	EC (µs/cm)	DO (Mg/l)	BOD (Mg/l)	CO ₃ (Mg/l)	HCO ₃ (Mg/l)	Cl (Mg/l)	Ca (Mg/l)	Mg (Mg/l)	TDS (Mg/l)
September	28 ± 0.00 ^c	7.0 ± 0.1 ^a	84.9 ± 9.7 ^{cd}	5.0 ± 0.20 ^d	21.5 ± 0.64 ^d	0.17 ± 0.03 ^d	18.6 ± 9.33 ^d	1.1 ± 0.57 ^b	24.0 ± 3.05 ^d	21.6 ± 2.51 ^b	5.67 ± 0.33 ^a
October	30.7 ± 0.00 ^b	6.5 ± 0.58 ^b	104.5 ± 2.8 ^c	2.73 ± 2.91 ^b	26.4 ± 0.69 ^b	6.47 ± 0.41 ^c	18.7 ± 1.24 ^d	0.2 ± 1.96 ^c	29.3 ± 2.67 ^c	0.767 ± 0.09 ^d	2.73 ± 2.13 ^c
November	30.0 ± 0.33 ^b	6.5 ± 0.03 ^b	99.8 ± 1.13 ^c	2.93 ± 1.76 ^a	27.7 ± 4.93 ^b	7.07 ± 0.23 ^c	16.5 ± 1.78 ^d	0.0 ± 0.0 ^d	41.3 ± 1.33 ^b	0.87 ± 0.67 ^d	5.33 ± 0.33 ^a
December	29.0 ± 0.33 ^{bc}	6.6 ± 0.28 ^b	72.2 ± 30.5 ^d	30.0 ± 1.12 ^a	26.2 ± 1.0 ^b	0.0 ± 0.00 ^e	49.3 ± 1.33 ^{bc}	0.97 ± 0.0 ^c	72.0 ± 0.15 ^e	19.2 ± 1.77 ^b	5.33 ± 0.33 ^a
January	28.0 ± 0.0 ^c	6.5 ± 0.05 ^b	128 ± 5.14 ^{bc}	6.17 ± 0.01 ^d	22.7 ± 0.32 ^{cd}	3.27 ± 4.81 ^a	45.5 ± 8.9 ^{bc}	0.2 ± 1.97 ^c	38.1 ± 10.7 ^{bc}	1.87 ± 0.41 ^{cd}	1.67 ± 0.33 ^{cd}
February	28.3 ± 0.33 ^c	6.5 ± 0.03 ^b	138 ± 3.96 ^a	6.83 ± 1.09 ^d	24.3 ± 4.33	0.23 ± 0.03 ^d	68.0 ± 4.0 ^{ab}	3.5 ± 1.37 ^a	25.3 ± 1.76 ^d	36.7 ± 0.33 ^a	0.93 ± 0.18 ^d
March	30.3 ± 0.33 ^b	6.6 ± 0.03 ^b	140.2 ± 0.6 ^a	2.73 ± 2.67 ^b	43.6 ± 4.45 ^a	7.6 ± 0.173 ^c	27.5 ± 1.00 ^c	0.27 ± 0.0 ^c	27.0 ± 4.0 ^c	2.63 ± 0.23 ^c	1.67 ± 0.33 ^{cd}
April	31.3 ± 0.33	6.6 ± 0.09 ^b	134 ± 3.28 ^{ab}	7.43 ± 0.09 ^c	24.0 ± 1.04 ^c	3.00 ± 2.31 ^b	35.6 ± 0.80	0.2 ± 1.96	77.3 ± 3.52 ^a	2.5 ± 0.153 ^c	1.53 ± 0.15 ^d
May	32 ± 0.58 ^a	6.6 ± 0.03 ^b	129 ± 1.87 ^{bc}	6.97 ± 0.12 ^d	24.5 ± 1.04 ^c	0.27 ± 0.03 ^d	58.7 ± 9.3 ^{ab}	1.9 ± 0.18 ^b	28 ± 1.15 ^c	36.4 ± 2.12 ^a	2.33 ± 0.33 ^c
June	29.7 ± 0.33 ^{bc}	6.6 ± 0.03 ^b	135 ± 0.95 ^{ab}	7.43 ± 0.37 ^c	23.5 ± 0.32	0.2 ± 0.096 ^d	77.3 ± 3.52 ^b	1.4 ± 0.12 ^b	34 ± 3.056 ^{bc}	36 ± 1.833 ^a	1.67 ± 0.33 ^{cd}
July	29.3 ± 0.33 ^{bc}	6.7 ± 0.06 ^{bc}	130 ± 0.79 ^{bc}	7.47 ± 0.20 ^c	22.7 ± 0.23 ^d	3.07 ± 0.67 ^b	33.2 ± 0.80 ^c	0.17 ± 0.0 ^c	85.3 ± 3.53 ^a	1.3 ± 0.058 ^{cd}	3.33 ± 0.33 ^b
August	27.7 ± 0.33 ^c	6.7 ± 0.03 ^{bc}	128 ± 0.72 ^b	7.2 ± 0.115 ^c	23 ± 0.26 ^{cd}	0.27 ± 0.03 ^d	90.7 ± 1.33 ^a	1.47 ± 0.1 ^b	33.3 ± 0.67 ^{bc}	32.4 ± 0.69 ^{ab}	2.33 ± 0.33 ^c
WHO Standard [17]	12–25	6.5–8.5	400	46	6	–S	125–350	500	100	150	500

Values were expressed as means ± SEM (Standard error of the means). Means having different superscripts (a, b, ab, bc, c, d, cd, or e) along the columns are significantly different at $p < 0.05$. T = Temperature, EC = Electrical Conductivity, DO = Dissolved Oxygen, BOD = Biological Oxygen Demands, TDS = Total Dissolve Solid, CO₃ = Carbonate ion, HCO₃ = Bicarbonate ion, Mg = Magnesium ion, Ca = Calcium ion, and Cl = Chloride ion.

Table 2. Concentrations of heavy metals in the water samples.

Month	Cd (mg/L)	Cu (mg/L)	Cr (mg/L)	Fe (mg/L)	Mn (mg/L)	Ni (mg/L)	Pb (mg/L)	Zn (mg/L)
September	0.01 ± 0.0 ^b	0.08 ± 0.01 ^a	0.03 ± 0.0 ^c	1.2 ± 0.07 ^a	0.7 ± 0.09 ^a	0.1 ± 0.1 ^a	0.0 ± 0.0 ^c	0.13 ± 0.02 ^a
October	0.01 ± 0.0 ^b	0.07 ± 0.01 ^a	0.03 ± 0.0 ^c	1.2 ± 0.04 ^a	0.68 ± 0.1 ^a	0.1 ± 0.1 ^a	0.0 ± 0.0 ^c	0.12 ± 0.0 ^{ab}
November	0.01 ± 0.0 ^b	0.06 ± 0.0 ^{ab}	0.02 ± 0.0 ^d	1.2 ± 0.03 ^a	0.73 ± 0.2 ^a	0.0 ± 0.0 ^b	0.0 ± 0.0 ^c	0.14 ± 0.0 ^a
December	0.003 ± 0.0 ^c	0.05 ± 0.1 ^{ab}	0.03 ± 0.0 ^c	1.4 ± 0.13 ^a	0.7 ± 0.14 ^a	0.0 ± 0.0 ^b	0.0 ± 0.0 ^c	0.1 ± 0.01 ^b
January	0.01 ± 0.0 ^b	0.2 ± 0.12 ^d	0.06 ± 0.0 ^a	0.4 ± 0.09 ^c	0.31 ± 0.1 ^b	0.0 ± 0.0 ^b	0.03 ± 0.0 ^b	0.0 ± 0.0 ^d
February	0.02 ± 0.0 ^a	0.3 ± 0.4 ^c	0.02 ± 0.0 ^d	0.1 ± 0.01 ^d	0.21 ± 0.0 ^c	0.1 ± 0.0 ^a	0.1 ± 0.0 ^a	0.0 ± 0.0 ^d
March	0.02 ± 0.0 ^a	0.4 ± 0.01 ^b	0.01 ± 0.0 ^e	0.34 ± 0.0 ^{bc}	0.3 ± 0.04 ^b	0.1 ± 0.0 ^a	0.02 ± 0.0 ^b	0.0 ± 0.0 ^d
April	0.01 ± 0.0 ^b	0.51 ± 0.0 ^{ab}	0.01 ± 0.0 ^e	0.4 ± 0.01 ^c	0.3 ± 0.04 ^b	0.01 ± 0.0 ^{ab}	0.03 ± 0.0 ^b	0.0 ± 0.0 ^d
May	0.627 ± 0.0 ^b	0.6 ± 0.02 ^{ab}	0.01 ± 0.0 ^e	0.42 ± 0.0 ^c	0.2 ± 0.02 ^c	0.0 ± 0.0 ^b	0.05 ± 0.0 ^{ab}	0.0 ± 0.0 ^d
June	0.01 ± 0.0 ^b	0.01 ± 0.0 ^d	0.05 ± 0.0 ^b	0.8 ± 0.07 ^b	0.2 ± 0.04 ^c	0.0 ± 0.0 ^b	0.06 ± 0.0 ^{ab}	0.0 ± 0.0 ^d
July	0.02 ± 0.0 ^a	0.03 ± 0.0 ^c	0.05 ± 0.0 ^b	1.1 ± 0.03 ^b	0.1 ± 0.01 ^d	0.0 ± 0.0 ^b	0.08 ± 0.0 ^a	0.0 ± 0.0 ^d
August	0.01 ± 0.0 ^b	0.03 ± 0.0 ^c	0.02 ± 0.0 ^d	0.98 ± 0.0 ^b	0.1 ± 0.00 ^d	0.0 ± 0.0 ^b	0.13 ± 0.0 ^a	0.0 ± 0.0 ^d
WHO Standard [17]	0.003	2.00	0.3	0.3	0.1–0.4	0.001	0.001	0.01–3

Values are expressed as means ± SEM (Standard error of the means). Means having different superscripts (a, b, ab, bc, c, d, or e) along columns are significantly different at $p < 0.05$. Cd = Cadmium, Cu = Copper, Cr = Chromium, Fe = Iron, Mn = Manganese, Ni = Nickel, Pb = Lead, and Zn = Zinc.

Figure 4 presents the STL decomposition of biochemical oxygen demand (BOD), breaking it into trend, seasonal, and residual components. The trend component reveals a mild upward movement, indicating a gradual increase in organic pollution levels over time. The

seasonal component shows clear periodic fluctuations, while the residuals remain relatively small and randomly distributed, confirming that the decomposition effectively captures the underlying structure in the BOD data.

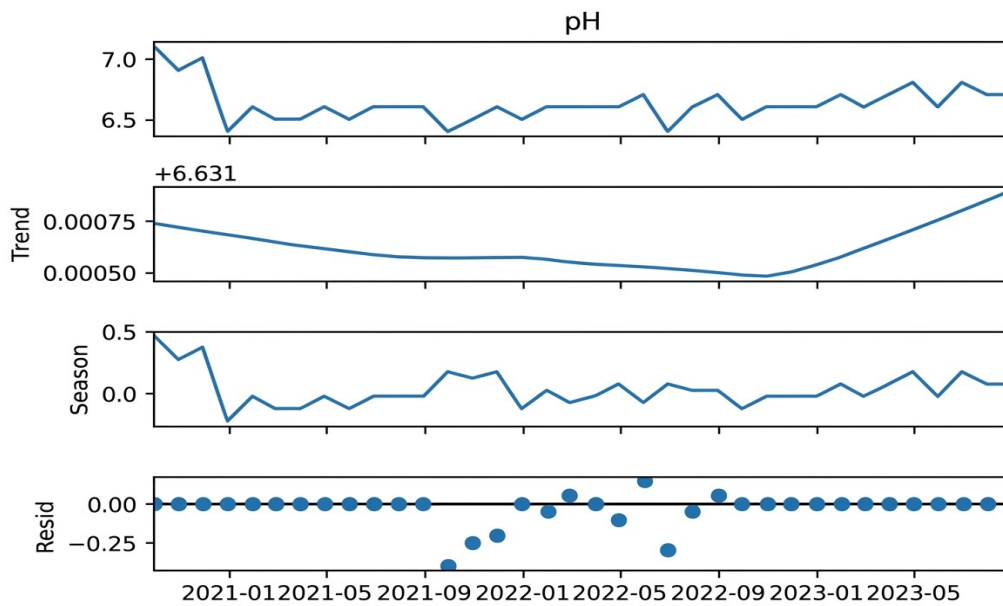


Figure 4. STL Plot for the decomposition of biochemical oxygen demand (BOD).

3.4. Seasonal and Trend Decomposition (SLT) in the Concentrations of Selected Heavy Metals from Jega River

Figure 5 illustrates the STL decomposition of copper (Cu) concentrations, breaking the time series into trend, seasonal, and residual components. The trend line appears relatively stable with minor variations, suggesting that

copper levels have remained fairly constant over the observed period. The seasonal component indicates periodic fluctuations likely influenced by environmental or anthropogenic activities, while the residuals are small and randomly dispersed, validating the model's ability to isolate the main patterns in the data.

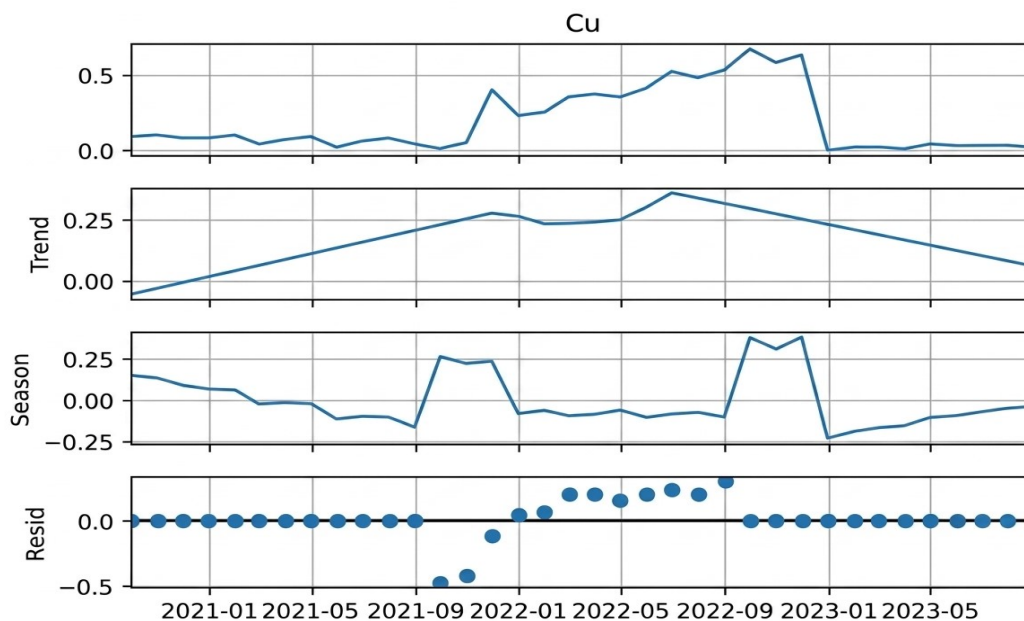


Figure 5. STL plot for the decomposition of copper (Cu).

Figure 6 presents the STL decomposition of nickel (Ni) concentrations, clearly separating the trend, seasonal, and residual components. The trend component shows a gradual decrease over time, indicating a potential long-term decline in nickel levels. The seasonal pattern remains evident, suggesting recurring environmental influences, while the residuals are minimal and randomly distributed, indicating the model adequately captures the variability in the data.

Figure 7 displays the STL decomposition of lead (Pb) concentrations into trend, seasonal, and residual components. The trend line appears relatively stable with minor fluctuations, indicating no substantial long-term increase or decrease in Pb levels. The seasonal component reveals recurring patterns across the periods, suggesting regular environmental or anthropogenic influences, while the residuals are minimal and evenly spread, indicating the model effectively captures the underlying structure in the data.

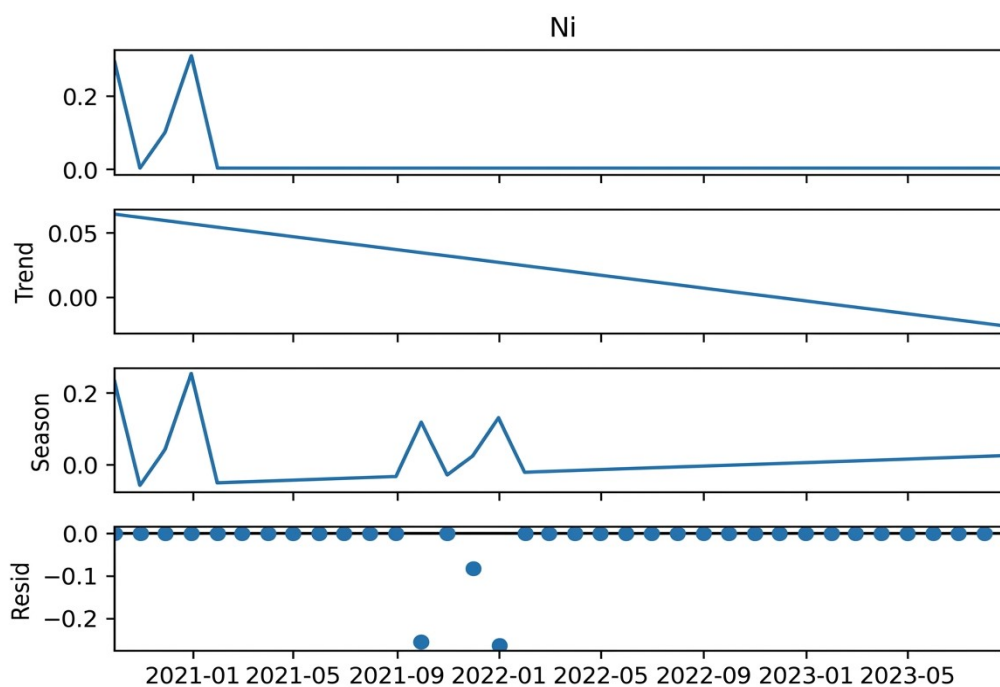


Figure 6. STL plot for the decomposition of nickel (Ni).

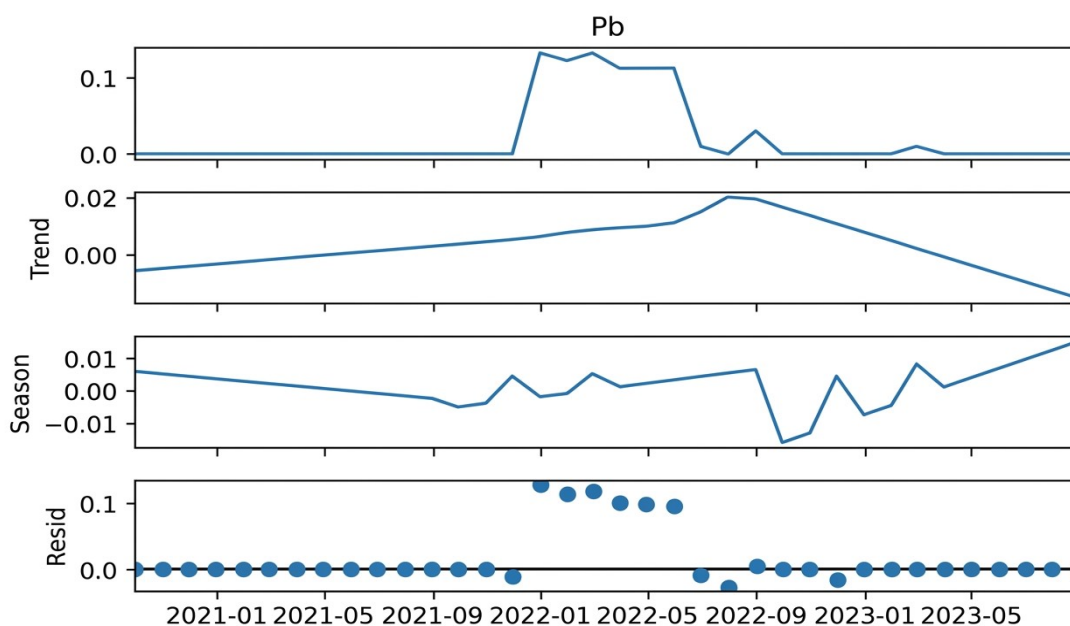


Figure 7. STL plot for the decomposition of lead (Pb).

3.5. Correlation Coefficient (r) among Physicochemical Parameters

Correlation coefficient (r) among the physicochemical parameters is shown in Table 3. Temperature showed a weak positive correlation (r = 0.313) with dissolved oxygen (DO), indicating a slight increase in DO levels as temperature rises. pH exhibited negative correlations with temperature, electrical conductivity (EC), and DO, suggesting that as pH decreases, temperature and EC tend to decrease, while DO levels tend to increase. Electrical conductivity (EC) showed a strong positive correlation with bicarbonate (HCO₃⁻) and a strong negative correlation with total dissolved solids (TDS), indicating that higher EC values are associated with higher HCO₃⁻ concentrations and lower TDS levels.

Dissolved oxygen (DO) shows positive correlations with electrical conductivity (EC) and biochemical oxygen

demand (BOD), suggesting that higher DO levels are associated with higher EC and BOD values. Biochemical oxygen demand (BOD) demonstrates positive correlations with EC, carbonate (CO₃²⁻), bicarbonate (HCO₃⁻), and chloride (Cl⁻), indicating a potential relationship between BOD (which represents organic pollution) and these chemical parameters. Calcium (Ca) exhibits a positive correlation with EC and a negative correlation with chloride (Cl⁻), suggesting that higher calcium levels correspond to higher EC values and lower chloride concentrations. Magnesium (Mg) shows a strong positive correlation with EC, indicating that higher magnesium concentrations are associated with higher EC levels. Total dissolved solids (TDS) have a strong negative correlation with EC, CO₃²⁻, HCO₃⁻, Cl⁻, Ca, and Mg, suggesting that as TDS levels increase, these parameters tend to decrease.

Table 3. Correlation coefficient (r) among physicochemical parameters.

	Temp	pH	EC	DO	BOD	CO ₃	HCO ₃	Cl	Ca	Mg	TDS
Temp	1										
pH	-0.381 0.022	1									
EC	0.087 0.613	-0.337 0.045	1								
DO	0.313 0.063	-0.383 0.021	0.491 0.002	1							
BOD	0.027 0.877	0.018 0.916	0.534 0.001	0.465 0.004	1						
CO ₃	0.031 0.857	0.025 0.885	0.590 0.000	0.068 0.694	0.629 0.000	1					
HCO ₃	-0.072 0.676	-0.086 0.620	0.792 0.000	0.513 0.001	0.456 0.005	0.367 0.028	1				
Cl	-0.072 0.679	-0.150 0.383	0.457 0.005	0.263 0.122	0.625 0.000	0.357 0.033	0.284 0.094	1			
Ca	-0.067 0.697	-0.235 0.167	0.369 0.027	0.262 0.123	0.033 0.849	0.031 0.858	0.410 0.013	-0.187 0.275	1		
Mg	0.089 0.606	-0.303 0.073	0.822 0.000	0.399 0.016	0.645 0.000	0.622 0.000	0.616 0.000	0.533 0.001	0.300 0.075	1	
TDS	0.068 0.694	0.162 0.345	-0.862 0.000	-0.376 0.024	-0.657 0.000	-0.577 0.000	-0.711 0.000	-0.632 0.000	-0.271 0.110	-0.816 0.000	1

Note: r = correlation coefficient; strength of correlation: Strong: 0.70–1.00 (positive), -0.70 to -1.00 (negative); Moderate: 0.40–0.69 (positive), -0.40 to -0.69 (negative); Weak: 0.10–0.39 (positive), -0.10 to -0.39 (negative); No correlation: r ≈ 0.

3.6. Correlation Coefficient (r) among Heavy Metals

Table 4 presents the correlation coefficients (r) among the heavy metals in the water samples. Copper (Cu) exhibited weak negative correlations with most of the metals, including Cd (r = -0.091), Cr (r = -0.425), Mn (r = -0.220), Ni (r = -0.143), and Pb (r = 0.322), while showing a negligible positive correlation with Zn (r = 0.051). Chromium (Cr) showed weak correlations with most metals, including Cd (r = 0.008), Fe (r = 0.196), Mn (r = -0.152), Ni (r = 0.044), Pb (r = -0.301), and Zn (r = -0.144), indicating

generally low associations. Iron (Fe) demonstrated a strong negative correlation with Cu (r = -0.716) and Pb (r = -0.645), and a moderate positive correlation with Mn (r = 0.469). Weak positive correlations were observed between Fe and Cd (r = 0.182), Ni (r = 0.317), and Zn (r = 0.288).

Manganese (Mn) showed a moderate positive correlation with Fe (r = 0.469) and Ni (r = 0.398), while weak correlations were observed with Cd (r = 0.069), Cu (r = -0.220), Cr (r = -0.152), Pb (r = -0.188), and Zn (r = 0.173). Nickel (Ni) exhibited weak positive correlations with Cd (r = 0.314), Fe (r = 0.317), Mn (r = 0.398), and Zn

($r = 0.254$), while weak negative correlations were observed with Cu ($r = -0.143$) and Pb ($r = -0.133$). Lead (Pb) showed a moderate negative correlation with Fe ($r = -0.645$) and weak correlations with other metals, including Cd ($r = 0.046$), Cu ($r = 0.322$), Cr ($r = -0.301$), Mn ($r = -0.188$),

Ni ($r = -0.133$), and Zn ($r = -0.367$). Zinc (Zn) exhibited weak correlations with all other metals, including Cd ($r = 0.074$), Cu ($r = 0.051$), Cr ($r = -0.144$), Fe ($r = 0.288$), Mn ($r = 0.173$), Ni ($r = 0.254$), and Pb ($r = -0.367$).

Table 4. Correlation coefficient (r) among heavy metals.

	Cd	Cu	Cr	Fe	Mn	Ni	Pb	Zn
Cd	1							
Cu	-0.091	1						
Cr	0.008	-0.425	1					
Fe	0.182	-0.716	0.196	1				
Mn	0.069	-0.220	-0.152	0.469	1			
Ni	0.314	-0.143	0.044	0.317	0.398	1		
Pb	0.046	0.322	-0.301	-0.645	-0.188	-0.133	1	
Zn	0.074	0.051	-0.144	0.288	0.173	0.254	-0.367	1

Note: r = correlation coefficient; strength of correlation: Strong: 0.70–1.00 (positive), -0.70 to -1.00 (negative); Moderate: 0.40–0.69 (positive), -0.40 to -0.69 (negative); Weak: 0.10–0.39 (positive), -0.10 to -0.39 (negative); No correlation: $r \approx 0$.

4. Discussion

This study assessed the safety and seasonal variation of water quality parameters in the Jega River, located in Kebbi State, Nigeria, over a 12-month period. The investigation was prompted by the lack of recent data on the river’s water quality, despite its critical role in supporting domestic, agricultural, and ecological functions. The analysis revealed that both physicochemical parameters and heavy metal concentrations displayed clear seasonal fluctuations. The observed pollution load in the river arises from a combination of anthropogenic and natural sources. The visible anthropogenic inputs include urban runoff carrying household and municipal wastes, agricultural runoff enriched with fertilizers, pesticides, and animal wastes, as well as direct human activities such as washing, bathing, and indiscriminate dumping of solid waste along the river banks. Additional contributions may stem from small-scale commercial activities, open defecation, and erosion induced by land-use changes within the catchment. Natural sources also play a significant role in background contamination. The weathering of underlying rocks and soils can release minerals and trace metals into the river system, particularly during the rainy season when runoff and leaching are intensified. Soil erosion, sediment transport, and dissolution of naturally occurring elements further contribute to variations in turbidity, nutrient levels, and metal concentrations. Seasonal hydrological processes, including dilution during peak rainfall and concentration during the dry season, also influence the overall water quality dynamics.

4.1. Physicochemical Parameters

The water temperature in the Jega River exhibited significant seasonal variation during the study period, with the highest temperature recorded in May (32.00 ± 0.58 °C)

and the lowest in August (27.71 ± 0.33 °C). This pattern aligns with typical seasonal trends observed in tropical river systems, where temperatures generally peak during the dry season due to increased solar radiation and reduced cloud cover [18]. Conversely, the cooler temperatures recorded during the wet season are likely due to increased rainfall, cloud cover, and runoff, which contribute to the cooling of surface waters. Precipitation induces cooling effects on temperature through cloud effects and evaporative cooling, particularly in arid and semi-humid regions [19]. Notably, water temperatures remained consistently above the World Health Organization’s (WHO) recommended limits for safe aquatic environments, posing potential ecological and public health risks. Elevated water temperatures can decrease dissolved oxygen levels, disrupt aquatic ecosystems, and impair the survival and reproduction of temperature-sensitive species. Moreover, high temperatures can promote harmful algal blooms, accelerate the proliferation of waterborne pathogens, and worsen existing water quality issues [20]. Prolonged exposure to such thermal stress can also lead to increased evaporation rates, which may reduce river flow and contribute to the desiccation of aquatic habitats [21].

The pH levels of the Jega River exhibited noticeable seasonal fluctuations, with the highest value recorded in September (7.00 ± 0.10) and the lowest in both October and February (6.50 ± 0.10 and 6.50 ± 0.03 , respectively). This trend is consistent with findings from previous studies, which have reported lower pH values during the rainy season due to increased surface runoff carrying organic matter and acidic compounds into the river system [22]. The influx of humic substances, carbonic acid from atmospheric CO₂, and organic acids from decaying vegetation can all contribute to a reduction in pH of water [23]. The observed variation in pH may be influenced by both natural processes, such as seasonal rainfall and decomposition of

organic matter, and anthropogenic activities, including agricultural runoff containing fertilizers and pesticides, which can alter the river's buffering capacity [24]. Despite these fluctuations, the pH levels remained within the acceptable range recommended by the World Health Organization for surface water (6.5–8.5), suggesting that the river water is unlikely to cause pH-related toxicity to aquatic life or humans under normal exposure conditions.

Electrical conductivity (EC) in the Jega River showed distinct seasonal variation, reaching its highest value in March ($140.20 \pm 0.60 \mu\text{S}/\text{cm}$) and dropping to its lowest in September ($84.90 \pm 9.70 \mu\text{S}/\text{cm}$). EC is primarily influenced by the concentration of dissolved ions such as calcium, magnesium, sodium, chloride, and sulfates in the water [25]. Elevated EC values during the dry season are commonly attributed to reduced water flow and increased evaporation, which concentrate these ions in the water column [26]. In contrast, the significant drop in EC observed during the wet season, particularly in September, is likely due to the dilution effect of increased rainfall and surface runoff, which lowers ion concentrations by increasing water volume [27]. Despite these fluctuations, the EC values throughout the study period remained within the permissible limits set by environmental and health agencies, indicating that the river water does not pose immediate risks in terms of salinity or ionic contamination.

Dissolved oxygen (DO) levels in the Jega River exhibited significant seasonal variation, with the highest concentration recorded in July ($7.47 \pm 0.20 \text{ mg}/\text{L}$) and the lowest in both October and March ($2.73 \pm 0.00 \text{ mg}/\text{L}$). This fluctuation can be attributed to changes in water temperature, microbial activity, and organic load. During the dry season, elevated temperatures increase microbial metabolism and biochemical processes, which consume more oxygen and result in decreased DO concentrations [28]. In contrast, cooler temperatures and enhanced aeration during the rainy season support higher DO levels [29]. The low DO levels observed in March coincided with a peak in biochemical oxygen demand (BOD) at $43.60 \pm 4.45 \text{ mg}/\text{L}$, indicating substantial organic pollution and a high rate of microbial decomposition. Elevated BOD reflects increased oxygen consumption by microorganisms breaking down organic matter, which further depletes available DO in the water [30]. Hypoxic conditions ($\text{DO} < 3 \text{ mg}/\text{L}$) pose serious ecological and public health concerns. They can lead to fish kills, reduced aquatic biodiversity, disruption of food webs, and degradation of water quality [31]. Prolonged hypoxia may progress to anoxia (complete oxygen depletion), which can result in the accumulation of toxic substances such as hydrogen sulfide and ammonia, further endangering aquatic life and rendering the water unsafe for human use [32]. Persistently low DO is a strong indicator of poor water quality and highlights the need for effective pollution control and wastewater management in the river catchment.

Biochemical oxygen demand (BOD) reached its highest level in March ($43.60 \pm 4.45 \text{ mg}/\text{L}$), indicating a substantial presence of organic matter undergoing microbial decomposition. This peak can be attributed to increased microbial activity during the dry season, when higher temperatures accelerate the breakdown of organic pollutants. Elevated BOD suggests a high organic load, likely originating from agricultural runoff, wastewater discharge, or decaying vegetation, all of which contribute to increased oxygen consumption in the water [33]. Similarly, carbonate (CO_3) concentrations peaked in March ($7.60 \pm 0.17 \text{ mg}/\text{L}$), suggesting an increase in the river's carbonate buffering capacity. This rise may be due to higher evaporation rates and the consequent concentration of dissolved minerals during the dry season, as well as potential inputs from weathering of carbonate-rich rocks [34]. Throughout the study period, BOD levels remained consistently above the recommended safety limits, posing potential risks to aquatic ecosystems. Excessively high BOD leads to excessive oxygen consumption as microorganisms break down organic matter, depleting dissolved oxygen (DO) and potentially resulting in hypoxic or even anoxic conditions. Severe oxygen depletion can disrupt aquatic ecosystems, cause fish kills, and promote the formation of toxic byproducts such as ammonia and hydrogen sulfide [35].

Total dissolved solids (TDS) in the Jega River exhibited notable seasonal variation, with the highest concentration recorded in September ($5.67 \pm 0.33 \text{ mg}/\text{L}$), during the peak of the wet season. This increase is likely due to heightened surface runoff and soil erosion, which transport a greater load of dissolved nutrients, organic matter, and minerals into the river system following heavy rainfall [36]. The influx of agricultural residues, domestic waste, and leachates from surrounding land can also contribute to elevated TDS during this period. Magnesium (Mg) concentrations peaked in May ($36.40 \pm 2.12 \text{ mg}/\text{L}$), aligning with the dry season. This may be attributed to reduced river flow and increased evaporation, which concentrates dissolved minerals, including magnesium, in the water. In addition, geological weathering of magnesium-rich rocks and possible inputs from agricultural or industrial sources may also contribute to the observed spike. Despite the seasonal fluctuations, TDS levels remained within the World Health Organization's permissible limits for surface water, indicating that the river water is not currently at risk of salinity-related issues.

4.2. Heavy Metals

Cadmium (Cd) concentrations were highest in May ($0.627 \pm 0.05 \text{ mg}/\text{L}$), which is consistent with studies that show increased heavy metal concentrations during dry periods due to reduced water volume and increased evaporation [36]. The increased concentration of Cd in the

water in dry season could have emanated from runoff from irrigation as farmers engage in intense dry farming around the river [36]. Conversely, copper (Cu) was highest in the dry season (May), which could be due to higher human activities such as agricultural runoff from irrigation and artisanal discharge during this period. The variation in copper concentrations between seasons could be explained by different sources of pollution, as agricultural chemicals and industrial effluents may contribute more during the dry season [37]. While Cu was within safe limits throughout the year, Cd concentrations exceeded safe limits except in December. This suggests Cd concentrations in the water may cause environmental and health risks. Cadmium toxicity leads to oxidative damage in fish, reducing their growth and spawning ability [38]. Human exposure may be related to various types of cancer, including breast, lung, prostate, nasopharynx, pancreas, and kidney cancers as well as liver and kidney problems and osteoporosis [39].

Chromium (Cr) concentrations were highest in January (0.06 ± 0.00 mg/L), while the lowest levels were recorded in March, April, and May (0.01 ± 0.00 mg/L). The variation in Cr concentrations could be attributed to both seasonal runoff patterns and local industrial activities, as Cr is commonly found in industrial effluents. Furthermore, there are artisanal activities such as welding and iron smelting close to the river which could be the source of Cr [4]. Similarly, manganese (Mn) was highest in November (0.73 ± 0.2 mg/L), which is consistent with findings from other studies that report increased manganese concentrations in rivers during the wet season, likely due to increased sediment and runoff [40]. Mn could have also emanated from leachate from landfill around the river [4]. Throughout the year, Cr was within safe limits while Mn was above permissible limits in the months of September, October, November, and December. Mn can bioaccumulate in aquatic organisms, leading to adverse physiological effects like oxidative stress and alterations in physiological parameters and immune function making them susceptible to diseases [41]. Chronic exposure may lead to its bioaccumulation in the liver which can cause liver damage in humans [41].

Nickel (Ni) concentrations were generally higher during the wet season, peaking at 0.08 ± 0.00 mg/L. This seasonal increase is likely due to the mobilization of Ni from soil and rocks by rainfall and its subsequent entry into the river system through runoff [42]. Metal scraps, a common occurrence around the river, could also be the source of Ni in the river [1]. Lead (Pb) also recorded its highest levels in the wet season (0.04 ± 0.05 mg/L), potentially resulting from increased surface runoff carrying pollutants from urban, vehicular, and industrial sources [35]. Lead acid batteries discarded in the city and around the river could also be the source of Pb in the water [1]. Zinc (Zn) followed a similar trend, with the highest concentrations observed in the wet season

(0.12 ± 0.11 mg/L), likely due to increased erosion, leaching from soils, and urban runoff during heavy rains. Zn concentrations remained within safe limits throughout the year, while Ni exceeded safe thresholds in February, March, April, September, and October. Pb concentrations surpassed permissible limits in all months except September through December. These findings highlight significant seasonal variation in metal concentrations and the potential ecological and health impacts of elevated Ni and Pb levels. Both metals are known to exert acute and chronic toxic effects on aquatic life, including inhibited growth, reproductive failure, enzymatic disruptions, and mortality. In fish and other aquatic organisms, Ni and Pb can damage critical organs such as gills (affecting respiration), kidneys (filtering waste), liver (metabolic function), and the nervous system [42]. Long-term human exposure may result in nephrotoxicity, neurotoxicity, cardiovascular issues, and developmental problems, particularly in children.

4.3. Correlation Coefficient (*r*) among the Parameters

The positive correlation coefficients observed between several physicochemical parameters and most heavy metals suggest that many of the pollutants in the water likely originate from common sources—such as industrial discharge, agricultural runoff, or urban waste—and may synergistically interact, thereby increasing ecological and public health risks. Of particular concern is the potential interaction between Cr and either Ni or Mn, which can significantly elevate the toxic potential of the water. Moreover, Ni can interact with Cr, enhancing oxidative stress and genotoxicity in aquatic organisms [43]. Similarly, Fe may interact with Mn, disrupting metabolic processes and enzyme activities [44]. Lead (Pb) has shown the ability to interact with Ni, exacerbating neurotoxicity and cellular damage, while zinc (Zn) may combine with copper (Cu), potentially affecting essential metal homeostasis in organisms [45]. These findings underscore the importance of evaluating not only the individual concentrations of heavy metals in water bodies but also their potential interactions, which can lead to amplified toxic effects. Such interactions can compromise aquatic ecosystem integrity, contaminate the food chain, and pose serious health risks to populations relying on such water sources.

The WHO drinking water standards were used as a conservative benchmark to evaluate potential human health risks. However, since the Jega River is a natural surface water body and not treated drinking water, these comparisons should be interpreted cautiously. Where applicable, the findings were also considered in relation to environmental quality standards for the protection of aquatic life.

One limitation of this study is the use of composited samples, which may obscure spatial heterogeneity among sampling locations (upstream, midstream, and downstream).

While this approach is suitable for assessing overall river water quality trends, future studies should consider site-specific analyses to better capture localized pollution sources and spatial variability.

5. Conclusions

This study evaluated the water safety of Jega River in Kebbi State, Nigeria, and revealed pronounced seasonal variations in physicochemical parameters and heavy metal concentrations. Several parameters exceeded World Health Organization (WHO) permissible limits, indicating that the river does not meet SDG 6.3 targets for improved water quality. These variations are largely driven by climatic factors, particularly rainfall, which influences river flow, dilution, sediment transport, and pollutant loading. During the wet season, elevated levels of nickel (Ni), lead (Pb), and zinc (Zn) were observed, likely due to surface runoff transporting contaminants from agricultural, urban, and industrial areas. In contrast, the dry season showed higher concentrations of cadmium (Cd), copper (Cu), manganese (Mn), and chromium (Cr), attributable to reduced water volume and limited dilution. Physicochemical parameters such as temperature, electrical conductivity (EC), dissolved oxygen (DO), biochemical oxygen demand (BOD), and magnesium (Mg) were also higher in the dry season, while pH and total dissolved solids (TDS) were elevated during the wet season. Importantly, temperature, DO, BOD, and heavy metals including Cd, Mn, Ni, and Pb exceeded recommended limits, posing risks to aquatic ecosystems and human health. Potential impacts include bioaccumulation, ecological disruption, and long-term health effects such as organ toxicity and carcinogenicity. Correlation analysis indicated significant relationships among parameters, suggesting common pollution sources and interactive effects. These findings highlight the need for continuous, seasonally targeted monitoring and effective pollution control measures, including regulation of industrial discharge, improved waste management, and sustainable agricultural practices. Strengthening policy implementation and increasing public awareness are also essential. Future research should identify pollution sources and assess long-term ecological and health impacts.

Author Contributions

A.I.: project administration, methodology, data curation, writing—original draft; I.O.: investigation, conceptualization, formal analysis, supervision; S.A.: formal analysis and visualization; T.Y.: supervision, writing—review and editing, and correspondence. All authors have read and agreed to the published version of the manuscript.

Funding

The research received no external funding.

Institutional Review Board Statement

Not applicable.

Informed Consent Statement

Not applicable.

Data Availability Statement

The data presented in this study are available on request from the corresponding author.

Conflicts of Interest

The authors declare no conflict of interest.

Use of AI and AI-assisted Technologies

During the preparation of this work, authors used ChatGPT and QuillBot to correct grammar and polish English. After using these tools, authors reviewed and edited the content as needed and take full responsibility for the content of the published article.

References

1. Yahaya, T.O.; Mohammed, U.F.; Umar, J.; et al. Level and Risk Assessment of Heavy Metal in Selected Leafy Vegetables Consumed in Birnin Kebbi, Northwestern Nigeria. *Savanna J. Basic Appl. Sci.* **2022**, *4*, 58–64. Available online: <https://www.sjbas.com.ng/single.php?journalId=151> (accessed on 25 October 2025).
2. Lukito, W. Current Evidence in Water and Hydration Science. *Ann. Nutr. Metab.* **2021**, *77*, 1–6.
3. Xiang, R.; Xu, Y.; Liu, Y.Q. Isolation Distance between Municipal Solid Waste Landfills and Drinking Water Wells for Bacteria Attenuation and Safe Drinking. *Sci. Rep.* **2019**, *9*, 17881.
4. Yahaya, T.; Oladele, E.; Chibs, B.; et al. Level and Health Risk Evaluation of Heavy Metals and Microorganisms in Urban Soils of Lagos, Southwest Nigeria. *Alger. J. Biosci.* **2020**, *1*, 51–60.
5. Gupta, G.K.; Liu, H.; Shukla, P. Pulp and Paper Industry–Based Pollutants, Their Health Hazards, and Environmental Risks. *Curr. Environ. Sci. Health* **2019**, *12*, 48–56.
6. Kuton, M.P.; Ayanda, I.O.; Uzoalu, I.U.; et al. Studies on Heavy Metals and Fish Health Indicators in *Malapterurus electricus* from Lekki Lagoon, Lagos, Nigeria. *Vet. Anim. Sci.* **2021**, *12*, 100169.
7. Lin, Q. Influence of Dams on River Ecosystem and Its Countermeasures. *J. Water Resour. Prot.* **2021**, *3*, 60–66.
8. Zarazua, G.; Ávila-Pérez, P.; Tejada, S.; et al. Analysis of Total and Dissolved Heavy Metals in Surface Water of a Mexican Polluted River by Total Reflection X-ray Fluorescence Spectrometry. *Spectrochim. Acta B At. Spectrosc.* **2022**, *61*, 1180–1184.
9. Yahaya, T.; Muhammed, A.; Onyeziri, J.A.; et al. Health Risks of Ecosystem Services in Ologe Lagoon, Lagos, Southwest Nigeria. *Pollution* **2022**, *8*, 681–692.

10. Winiarska, M.A.; Kowalczyk-Vasilev, E.; Kwiatkowska, K.; et al. Dietary Intake and Content of Cu, Mn, Fe, and Zn in Selected Cereal Products Marketed in Poland. *Biol. Trace Elem. Res.* **2019**, *187*, 568–578.
11. Yahaya, T.O.; Abdulganiyu, Y.; Ologe, O.; et al. Quality and Safety Assessment of Borehole Water around Simpson Transfer Loading Station in Lagos, Southwest Nigeria. *Dutse J. Pure Appl. Sci.* **2022**, *8*, 20–35.
12. Farmer, F.Y.; Sun, S.; Duan, X. Refined Assessment of Exposure and Health Risks of Heavy Metals in Water for the Children in Xigu District, Lanzhou. *Environ. Sci.* **2020**, *41*, 262–272.
13. Sim, S.F.; Ling, T.Y.; Nyanti, L.; et al. Assessment of Heavy Metals in Water, Sediment, and Fishes of a Large Tropical Hydroelectric Dam in Sarawak, Malaysia. *J. Chem.* **2016**, *2016*, 8923183.
14. Preonty, N.; Hassan, N.; Reza, S.; et al. Pollution and Health Risk Assessment of Heavy Metals in Surface Water of the Industrial Region in Gazipur, Bangladesh. *Environ. Chem. Ecotoxicol.* **2025**, *7*, 527–538.
15. Wei, G.L.; Yang, Z.F.; Cui, B.S. Impact of Dam Construction on Water Quality and Water Self-Purification Capacity of the Lancang River, China. *Water Resour. Manag.* **2009**, *23*, 1763–1780.
16. APHA. Standard Methods for the Examination of Water and Wastewater 24. Available online: <https://secure.apha.org/imis/ItemDetail?iProductCode=978-087553-2998&CATEGORY=BK> (accessed on 25 October 2025).
17. WHO. Guidelines for Drinking-Water Quality Fourth Edition Incorporating the First and Second Addenda. Available online: <https://www.who.int/publications/i/item/9789240045064> (accessed on 24 October 2025).
18. Echebima, S.I.; Obafemi, A.A. The Influence of Local Rainy and Dry Seasons on the Diurnal Temperature Range in Nigeria. *Atmos. Clim. Sci.* **2023**, *13*, 314–332.
19. Chen, C.; Wang, S.; Wang, Z.; et al. Differential Impacts of Sub-Daily Precipitation on Temperature Extremes Across China's Climatic Zones. *Geophys. Res. Lett.* **2025**, *52*, e2024GL114088.
20. Bolan, S.; Padhye, L.P.; Jasemizad, T.; et al. Impacts of Climate Change on the Fate of Contaminants through Extreme Weather Events. *Sci. Total Environ.* **2024**, *909*, 168388.
21. Johnson, M.F.; Albertson, L.K.; Algar, A.C.; et al. Rising Water Temperature in Rivers: Ecological Impacts and Future Resilience. *WIREs Water* **2024**, *11*, e1724.
22. Nnaemeka-Okeke, R.C.; Okeke, F.O. Assessing the Influence of Seasonal Precipitation Patterns on Groundwater Quality in the Coal Rich Environment of Enugu, Nigeria. *Discov. Appl. Sci.* **2024**, *6*, 208.
23. Muhib, M.I.; Kabir, M.H. Should Optimum pH Range for Different Surface Water Become Fluctuate with Usage and Condition in Perspective of Aquatic Environment and Human Health Effects? *Am. Int. J. Nurs. Educ. Pract.* **2021**, *2*, 19–22.
24. Mansour, H.; Ahmed, S.A.; Zaghloul, A.; et al. Seasonal Variation Effect on Water Quality and Sediments Criteria and Its Influence on Soil Pollution: Fayoum Governorate, Egypt. *Environ. Sci. Eur.* **2024**, *36*, 132.
25. Rebello, L.R.B.; Siepman, T.; Drexle, S. Correlations between TDS and Electrical Conductivity for High-Salinity Formation Brines Characteristic of South Atlantic Pre-Salt Basins. *Water SA* **2020**, *46*, 602–609.
26. Gupta, D.; Ranjan, R.J.; Parthasarathy, P.; et al. Spatial and Seasonal Variability in the Water Chemistry of Kabar Tal Wetland (Ramsar Site), Bihar, India: Multivariate Statistical Techniques and GIS Approach. *Water Sci. Technol.* **2021**, *83*, 2100–2117.
27. Allia, Z.; Lalaoui, M.; Chebbah, M. Spatial and Seasonal Assessment of Surface Water Quality for Domestic Use in a Semi-Arid Area of the Upper Kebir Sub-Basin, NE Algeria. *Water Supply* **2024**, *24*, 2946–2962.
28. Bonacina, L.; Fasano, F.; Mezzanotte, V.; et al. Effects of Water Temperature on Freshwater Macroinvertebrates: A Systematic Review. *Biol. Rev. Camb. Philos. Soc.* **2023**, *98*, 191–221.
29. Siddique, M.A.; Mahalder, B.; Haque, M.M.; et al. Impact of Climatic Factors on Water Quality Parameters in Tilapia Broodfish Ponds and Predictive Modeling of Pond Water Temperature with ARIMAX. *Heliyon* **2024**, *10*, e37717.
30. Vigiak, O.; Grizzetti, B.; Udias-Moinelo, A.; et al. Predicting Biochemical Oxygen Demand in European Freshwater Bodies. *Sci. Total Environ.* **2019**, *666*, 1089–1105.
31. Breitburg, D. Effects of Hypoxia, and the Balance between Hypoxia and Enrichment, on Coastal Fishes and Fisheries. *Estuaries* **2002**, *25*, 767–781.
32. Larance, S.; Wang, J.; Delavar, M.A.; et al. Assessing Water Temperature and Dissolved Oxygen and Their Potential Effects on Aquatic Ecosystem Using a SARIMA Model. *Environments* **2025**, *12*, 25.
33. Maddah, H.A. Predicting Optimum Dilution Factors for BOD Sampling and Desired Dissolved Oxygen for Controlling Organic Contamination in Various Wastewaters. *Int. J. Chem. Eng.* **2022**, *2022*, 8637064.
34. Lemessa, F.; Simane, B.; Seyoum, A.; et al. Assessment of the Impact of Industrial Wastewater on the Water Quality of Rivers around the Bole Lemi Industrial Park (BLIP), Ethiopia. *Sustainability* **2023**, *15*, 4290.
35. Edegbene, A.O.; Yandev, D.; Omotehinwa, T.O.; et al. Water Quality Assessment in Benue South, Nigeria: An Investigation of Physico-Chemical and Microbial Characteristics. *Water Sci.* **2025**, *39*, 279–290.
36. Edward, A.; Adamu, N. Dry and Wet Seasonal Levels of Heavy Metals in Water, Fish (*Brycinus leuciscus*) and Sediments from Kiri Reservoir in Shelleng Local Government, Adamawa State, Nigeria. *J. Agric. Aquac.* **2023**, *5*, 1–7.
37. Singh, J.; Pant, M.; Ghoshal, T.; et al. Spatio-Seasonal Observations of Water Quality Index, Heavy-Metal Pollution Index and Microbial Contagion in Springs of Lower Indian Himalayan Zone. *Environ. Claims J.* **2025**, *37*, 1–36.
38. Liu, Y.; Chen, Q.; Li, Y.; et al. Toxic Effects of Cadmium on Fish. *Toxics* **2022**, *10*, 622.

39. Genchi, G.; Sinicropi, M.S.; Lauria, G.; et al. The Effects of Cadmium Toxicity. *Int. J. Environ. Res. Public Health* **2020**, *17*, 3782.
40. Gödeke, S.H.; Jamil, H.; Schirmer, M.; et al. Iron and Manganese Mobilisation Due to Dam Height Increase for a Tropical Reservoir in South East Asia. *Environ. Monit. Assess.* **2022**, *194*, 358.
41. Wang, Q.G.; Du, Y.H.; Su, Y.; et al. Environmental Impact Post-Assessment of Dam and Reservoir Projects: A Review. *Procedia Environ. Sci.* **2022**, *13*, 1439–1443.
42. Cuevas, J.G.; Faz, A.; Martínez-Martínez, S.; et al. Influence of Rainfall on Physicochemical Characteristics of Runoff Water and Sediments in Riverbeds Affected by Mining and Agricultural Activities. *Sci. Total Environ.* **2025**, *958*, 177889.
43. Yahaya, T.O.; Bashar, D.M.; Liman, U.U.; et al. Effects of Pit Latrines on Borehole and Well Water in Maryland, Lagos, Nigeria. *J. Adv. Environ. Health Res.* **2023**, *11*, 20–27.
44. Costa, M.; Salnikow, K.; Sutherland, J.E.; et al. The Role of Oxidative Stress in Nickel and Chromate Genotoxicity. *Mol. Cell. Biochem.* **2002**, *234–235*, 265–275.
45. Redha, A.; Al-Hasan, R.; Afzal, M. Synergistic and Concentration Dependent Toxicity of Multiple Heavy Metals Compared with Single Heavy Metals in *Conocarpus lancifolius*. *Environ. Sci. Pollut. Res. Int.* **2021**, *28*, 23258–23272.